2010 IEEE International Conference on Robotics and Automation
Anchorage Convention District
May 3-8, 2010, Anchorage, Alaska, USA

Differentially Flat Mobile Manipulators Mounted with an Under-actuated Vertical Arm

Ji-Chul Ryu and Sunil K. Agrawal

Abstract— **This paper discusses how mobile manipulators with an under-actuated vertical arm can be designed to be differentially flat. The property of differential flatness is achieved by appropriate inertia redistribution of the vertical arm and a wide range of under-actuation becomes possible. As a result of having the flatness property, the under-actuated mobile manipulators are capable of executing point-to-point maneuvers as mobile manipulators with a fully actuated arm would do. In addition, the trajectory planning and feedback controller design for point-to-point motions in state space is considerably simplified despite the under-actuation of the arm and nonholonomic constraints (from no-slip assumption) of the mobile base, which make the system more difficult to plan and control. These ideas are demonstrated through an illustrative example of a mobile manipulator consisting of an under-actuated vertical three-link arm and a two-wheeled differentially driven mobile base using differential flatness.**

I. INTRODUCTION

Mobile manipulators are one of the most active research areas in robotics since they have a wide spectrum of practical applications including mobility assistance, material handling, and military missions such as bomb disposal. While mobile manipulators are usually designed with a fully actuated arm, i.e., actuators are placed at every joint in the arm, under-actuation can be a viable solution to reduce the manufacturing and operating costs, or to improve reliability in case of actuator failure. A mobile manipulator with an unactuated joint was addressed in [1] and an under-actuated n-link manipulator with a fixed base was discussed in [2]. However, in these references, only one joint was allowed to be unactuated in their system.

Despite the under-actuation, which makes the system more difficult to plan and control, it was shown in the authors' previous studies [3], [4] that using the differential flatness theory mobile manipulators can be designed to be capable of executing point-to-point maneuvers as a mobile manipulator with a fully actuated arm would do and in addition, a wide range of under-actuation is possible.

Whereas the mobile manipulators discussed in [3], [4] operate in a horizontal plane, in this paper, *differential flatness has been investigated in the context of a mobile manipulator mounted with an under-actuated arm that operates in a vertical plane*. In this system, like in the previous studies, the differential flatness property is achieved by inertia redistribution with addition of torsional springs at unactuated joints. Through an illustrative example of an under-actuated vertical three-link mobile manipulator with a two-wheeled differentially driven mobile base, it is demonstrated that the trajectory planning and feedback controller design problem can be solved in an efficient and simplified way using differential flatness.

The authors are with the Department of Mechanical Engineering, University of Delaware, Newark, DE 19716 jcryu, agrawal@udel.edu

The rest of this paper is organized as follows: In Section II, the dynamic model of a mobile manipulator with an n-link vertical arm is derived. In Section III, design methodology for differential flatness is adopted and the flatness property is investigated by exploiting the special structure of the governing equations. The simulation results of an under-actuated mobile manipulator with a vertical three-link manipulator arm are provided in Section IV.

II. DYNAMIC MODEL DERIVATION

In this section, we derive the equations of motion of a mobile manipulator consisting of a mobile base and an n-link vertical manipulator arm as shown in Fig. 1. The mobile base moves in a horizontal plane while the manipulator arm operates in a vertical plane attached to the mobile base. We model the mobile base as a two-wheeled differentially driven robot. The manipulator is mounted on the mobile base at P_1 through a revolute joint. The point P_1 is off the midpoint O between the two wheels by a distance d. The center of mass C of the mobile base is at a distance a from the midpoint. The system's configuration is given by

$$\mathbf{q} = [\mathbf{q_A}^T,\ \mathbf{q_B}^T]^T, \tag{1}$$

where $\mathbf{q_A} = [x,\ y,\ \theta]^T$ and $\mathbf{q_B} = [\theta_1,\ \theta_2,\ \cdots,\ \theta_n]^T$. $\mathbf{q_A}$ are the coordinates describing the mobile base's position and orientation. $\mathbf{q_B}$ are the joint angles for the manipulator arm. (x, y) is the position of midpoint O of the mobile base and θ is the orientation of the mobile base with respect to the x-axis. θ_i denotes the relative joint angle of link i of the arm with respect to link $i-1$. l_i and l_{ci} represent the length of link i and the distance of the center of mass of link i from joint P_i, respectively.

To derive the equations of motion of the mobile manipulator system, we first find the equations of motion for the mobile base and the manipulator arm separately, with interaction forces and torques in the two submodels. These subsystem models are then combined together and the interaction forces and torques are eliminated to find the equations of motion of the entire system.

A. Dynamic Model of the Mobile Base

From the assumption of no-slip on the wheels, the nonholonomic constraint on the system coordinates is given by

$$\mathbf{C_A}(\mathbf{q_A})\dot{\mathbf{q}}_\mathbf{A} = 0, \tag{2}$$

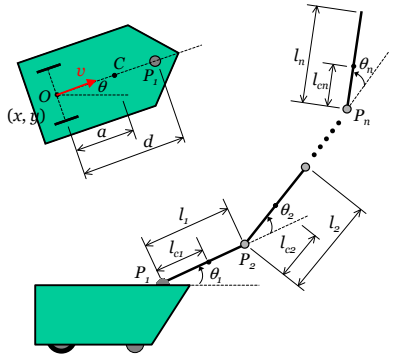

Fig. 1. A mobile manipulator consisting of a mobile base and an n-link vertical manipulator arm mounted on the base. The configuration of the system is described by $(x, y, \theta, \theta_1, \cdots, \theta_n)$.

where $\mathbf{C_A}(\mathbf{q_A}) = [\sin\theta, -\cos\theta, 0]$. With a matrix $\mathbf{S_A}(\mathbf{q_A})$ that spans the null space of $\mathbf{C_A}(\mathbf{q_A})$, it is possible to define a velocity vector $\boldsymbol{\nu_A} = [v,\ \dot{\theta}]^T$ such that

$$\dot{\mathbf{q}}_\mathbf{A} = \mathbf{S_A}(\mathbf{q_A})\boldsymbol{\nu_A},\ \text{where}\ \mathbf{S_A}(\mathbf{q_A}) = \begin{pmatrix} \cos\theta & 0 \\ \sin\theta & 0 \\ 0 & 1 \end{pmatrix}. \quad (3)$$

Here, v is the velocity of the midpoint O (Figure 1). Using Lagrange formulation with the multiplier vector $\boldsymbol{\lambda}$ associated with the constraint of (2), the equations of motion for the mobile base are given by

$$\mathbf{M_A}\ddot{\mathbf{q}}_\mathbf{A} + \mathbf{V_A} = \mathbf{E_A}\boldsymbol{\tau_A} - \mathbf{C_A^T}\boldsymbol{\lambda} - \mathbf{R}, \quad (4)$$

where $\mathbf{R}$ is the 3-dimensional generalized force vector along $\mathbf{q_A}$ due to the interaction forces and moments applied by the manipulator arm on the mobile robot at P_1. The structures of the terms in the above equation are

$$\mathbf{M_A} = \begin{pmatrix} m_0 & 0 & -am_0\sin\theta \\ 0 & m_0 & am_0\cos\theta \\ -am_0\sin\theta & am_0\cos\theta & a^2m_0 + I_0 \end{pmatrix}, \boldsymbol{\tau_A} = \begin{pmatrix} \tau_r \\ \tau_l \end{pmatrix},$$

$$\mathbf{V_A} = \begin{pmatrix} -am_0\dot{\theta}^2\cos\theta \\ -am_0\dot{\theta}^2\sin\theta \\ 0 \end{pmatrix}, \mathbf{E_A} = \begin{pmatrix} \cos\theta/r & \cos\theta/r \\ \sin\theta/r & \sin\theta/r \\ b/r & -b/r \end{pmatrix}.$$

Here, m_0 is the mass and I_0 the moment of inertia of the mobile base about its center of mass. r is the radius of the robot's wheels and b is the half the distance between the two wheels. τ_r and τ_l are the motor torques applied on the robot's right and left wheels, respectively.

B. Dynamic Model of the Manipulator Arm

The dynamic equations of the manipulator arm can be derived using Lagrange's formulation. The kinetic energy of link i of the manipulator is given by

$$K_i = \frac{1}{2}m_i\mathbf{v}_{ci}^T\mathbf{v}_{ci} + \frac{1}{2}\boldsymbol{\omega}_i^T\mathbf{I}_i\boldsymbol{\omega}_i, \quad (5)$$

where m_i is the mass of link i, $\mathbf{v}_{ci}$ is the velocity of the center of mass of link i, $\mathbf{I}_i$ is the moment of inertia matrix of link i with respect to the coordinate frame attached to the body given by $\mathbf{I}_i$ = diag(I_{xi}, I_{yi}, I_{zi}). $\boldsymbol{\omega}_i$ is the inertial angular velocity of link i given by

$$\boldsymbol{\omega}_i = \dot{\theta}\hat{\mathbf{z}} + (\dot{\theta}_1 + \dot{\theta}_2 + \cdots + \dot{\theta}_i)\hat{\mathbf{u}}, \quad (6)$$

where $\hat{\mathbf{z}}$ is the unit vector along an axis normal to the horizontal plane in which the mobile base moves. $\hat{\mathbf{u}}$ is the unit vector normal to the vertical plane in which the manipulator arm operates. The equations of motion of the manipulator can be written as

$$\mathbf{M_B}(\mathbf{q})\ddot{\mathbf{q}} + \mathbf{B_B}(\mathbf{q}, \dot{\mathbf{q}})\dot{\mathbf{q}} + \mathbf{G_B}(\mathbf{q}) = \mathbf{Q_B}, \quad (7)$$

where $\mathbf{M_B}(\mathbf{q})$ denotes the $(n+3)\times(n+3)$ inertia matrix and $\mathbf{B_B}(\mathbf{q}, \dot{\mathbf{q}})\dot{\mathbf{q}}$ the $(n+3)$-dimensional Coriolis and centripetal vector. The $(n+3)$-dimensional gravity vector $\mathbf{G_B}$ is related to the potential energy V as $\mathbf{G_B} = \frac{\partial V}{\partial \mathbf{q}}$. $\mathbf{Q_B}$ is the $(n+3)$-dimensional vector of generalized forces on the manipulator given by

$$\mathbf{Q_B} = \begin{pmatrix} \mathbf{R} \\ \boldsymbol{\tau_B} \end{pmatrix}, \quad (8)$$

where $\boldsymbol{\tau_B} = [\tau_1, \tau_2, \cdots, \tau_n]^T$ and τ_i $(i = 1, ..., n)$ denotes the torque input at joint i.

C. Dynamic Model of the Mobile Manipulator

From (3), the rates in the entire system satisfy the following relation, with $\boldsymbol{\nu} = [\boldsymbol{\nu}_\mathbf{A}^T,\ \dot{\mathbf{q}}_\mathbf{B}^T]^T$,

$$\dot{\mathbf{q}} = \mathbf{S}\boldsymbol{\nu},\ \text{where}\ \mathbf{S} = \begin{pmatrix} \mathbf{S_A} & \mathbf{0} \\ \mathbf{0} & \mathbf{I_n} \end{pmatrix}. \quad (9)$$

Here, $\mathbf{I_n}$ denotes the identity matrix of size n.

On combining (4) and (7), one gets

$$\mathbf{M}(\mathbf{q})\ddot{\mathbf{q}} + \mathbf{V}(\mathbf{q}, \dot{\mathbf{q}}) + \mathbf{G_B}(\mathbf{q}) = \mathbf{E}(\mathbf{q})\boldsymbol{\tau} - \begin{pmatrix} \mathbf{C_A^T}\boldsymbol{\lambda} \\ \mathbf{0} \end{pmatrix}, \quad (10)$$

where $\mathbf{M}(\mathbf{q})$ denotes the $(n+3)\times(n+3)$ inertia matrix, $\mathbf{V}(\mathbf{q}, \dot{\mathbf{q}})$ the $(n+3)\times 1$ Coriolis and centripetal vector, and

$$\mathbf{E} = \begin{pmatrix} \mathbf{E_A} & \mathbf{0} \\ \mathbf{0} & \mathbf{I_n} \end{pmatrix},\ \boldsymbol{\tau} = \begin{pmatrix} \boldsymbol{\tau_A} \\ \boldsymbol{\tau_B} \end{pmatrix}.$$

By differentiating (9), one obtains $\ddot{\mathbf{q}} = \dot{\mathbf{S}}\boldsymbol{\nu} + \mathbf{S}\dot{\boldsymbol{\nu}}$. On substituting $\ddot{\mathbf{q}}$ into (10), premultiplying by $\mathbf{S}^T$, and using the property $\mathbf{C_A}\mathbf{S_A} = \mathbf{0}$, one finally gets

$$\mathbf{A}(\mathbf{q})\dot{\boldsymbol{\nu}} + \mathbf{D}(\mathbf{q}, \boldsymbol{\nu}) + \mathbf{G}(\mathbf{q}) = \mathbf{S^T}\mathbf{E}\boldsymbol{\tau}, \quad (11)$$

where $\mathbf{A}(\mathbf{q}) = \mathbf{S^T}\mathbf{M}\mathbf{S}$, $\mathbf{D}(\mathbf{q}, \boldsymbol{\nu}) = \mathbf{S^T}\mathbf{M}\dot{\mathbf{S}}\boldsymbol{\nu} + \mathbf{S^T}\mathbf{V}$ and $\mathbf{G}(\mathbf{q}) = \mathbf{S}^T\mathbf{G_B}$. Note that $\mathbf{A}(\mathbf{q})$ is an $(n+2)\times(n+2)$ inertia matrix and $\mathbf{D}(\mathbf{q}, \boldsymbol{\nu})$ and $\mathbf{G}(\mathbf{q})$ are $(n+2)$-dimensional vectors. Due to the structure of matrix $\mathbf{S}$ as described in (9) and the fact that the potential energy V is independent of $\mathbf{q_A}(= [x\ y\ \theta]^T)$, the first two entries of $\mathbf{G}(\mathbf{q})$ are zero.

In general, the dynamic model of a mobile manipulator is highly nonlinear. Hence, it is quite difficult to characterize the differential flatness of such a system if it is underactuated. In the next section, a set of design conditions will be identified such that the mobile manipulator system becomes differentially flat.

III. Differentially Flat Design of Under-actuated mobile Manipulator

In the previous studies [3], [4], we showed that the mobile manipulators with an under-actuated planar manipulator arm that operates in a horizontal plane can be made to be differentially flat if the inertia distribution within the manipulator arm is properly chosen. In this paper, motivated by these studies, we adopt the following design conditions for the mobile manipulator. The inertia distribution of the arm is chosen in the following way: (i) the center of mass of the last link n of the arm is selected to lie on the last joint axis n, (ii) the center of mass of the last two links n and $n-1$ lies on the joint axis $n-1$, (iii) this procedure repeats until the center of mass of the last j links, i.e., n, $n-1$, ..., $n-j+1$, lies on the joint axis $n-j+1$. These design conditions can be practically achieved in a physical design by counter balancing or by properly locating the actuators in the mechanical arm [5], [6].

With these design conditions, we consider the under-actuation in the manipulator to be as follows: The first $n-j+1$ joints have actuators while the remaining $j-1$ joints, i.e., joints $n-j+2$ through n, are unactuated. These joints are mounted with torsion springs. In this case, the manipulator arm is under-actuated by $j-1$ and $\boldsymbol{\tau_B}$ has a special form of $\boldsymbol{\tau_B} = [\tau_1, \tau_2, \cdots, \tau_{n-j+1}, 0, \cdots, 0]^T$. The contribution of the torsion springs to the potential energy, if added to each of the last $j-1$ joints, is

$$V_s = \sum_{i=n-j+2}^{n} \frac{1}{2} k_i \theta_i^2. \tag{12}$$

On the other hand, the potential energy due to gravitation, V_g, which is the sum of the potential energy of each link, is independent of the last j joint coordinates, $\theta_{n-j+1}, ..., \theta_n$ due to the special design method. The total potential energy of the system is given by $V = V_s + V_g$. By taking the value of j from 2 to n, a wide range of under-actuation is possible. Later, it will be shown that the dynamic model of each mobile manipulator with under-actuated joints corresponding to the different value of j is differentially flat.

A. Structure of Equations of Motion

It can be shown that the equations of motion of the mobile manipulator, with the proposed inertia distribution has the following structure.

$$\mathbf{A}_j(\mathbf{q})\dot{\boldsymbol{\nu}} + \mathbf{D}_j(\mathbf{q}, \boldsymbol{\nu}) + \mathbf{G}_j(\mathbf{q}) = \begin{pmatrix} \mathbf{S_A^T E_A} \boldsymbol{\tau_A} \\ \boldsymbol{\tau_B} \end{pmatrix}. \tag{13}$$

In the above model, the subscript j indicates that the special inertia distribution is applied on the last j links as j can vary from 2 to n. For each choice of j, the $(n+2)\times(n+2)$ inertia matrix $\mathbf{A}_j$ and the $(n+2)$-dimensional nonlinear vector $\mathbf{D}_j$ take the following special form:

$$\mathbf{A}_j = \begin{pmatrix} & & & & 0 & 0 & \cdots & 0 \\ & & & & 0 & 0 & \cdots & 0 \\ & \bar{\mathbf{A}}_j(\mathbf{q}) & & & a_{n-j+3} & a_{n-j+4} & \cdots & a_{n+2} \\ & & & & \vdots & \vdots & \vdots & \vdots \\ 0 & 0 & a_{n-j+3} & \cdots & a_{n-j+3} & a_{n-j+4} & \cdots & a_{n+2} \\ 0 & 0 & a_{n-j+4} & \cdots & a_{n-j+4} & a_{n-j+4} & \cdots & a_{n+2} \\ \vdots & \vdots & \vdots & \cdots & \vdots & \vdots & \ddots & \vdots \\ 0 & 0 & a_{n+2} & \cdots & a_{n+2} & a_{n+2} & ... & a_{n+2} \end{pmatrix}, \tag{14}$$

$$\mathbf{D}_j = \begin{pmatrix} d_1(\mathbf{q}, \boldsymbol{\nu}) \\ d_2(\mathbf{q}, \boldsymbol{\nu}) \\ d_3(\mathbf{q}, \boldsymbol{\nu}) \\ \\ \vdots \\ \\ \vdots \\ \\ d_{n+2}(\mathbf{q}, \boldsymbol{\nu}) \end{pmatrix}, \ \mathbf{G}_j = \begin{pmatrix} 0 \\ 0 \\ g_3(\bar{\mathbf{q}}) \\ \vdots \\ g_{n-j+2}(\bar{\mathbf{q}}) \\ 0 \\ k_{n-j+2}\theta_{n-j+2} \\ \vdots \\ k_n \theta_n \end{pmatrix}. \tag{15}$$

Here, $\bar{\mathbf{q}}$ is a vector containing the joint variables θ_1 through θ_{n-j}. $\bar{\mathbf{A}}_j(\mathbf{q})$ is the $(n-j+2)\times(n-j+2)$ submatrix of $\mathbf{A}_j$. Due to the choice of inertia distribution, all terms in $\mathbf{A}_j$, except for its submatrix $\bar{\mathbf{A}}_j$, are constants. In addition, the matrix $\mathbf{A}_j$ has the structure of a reflected $\mathbf{L}$ pattern. For example, the $(n+2)$th row and $(n+2)$th column have all the same constants a_{n+2}, except for their first two elements which are 0. $g_i (i = 3, ..., n-j+2)$ is the entry of $\mathbf{G}$ in (11).

B. Differential Flatness

Under this special inertia distribution and under-actuation, the equations of motion of the system is given by $n+2$ first-order dynamic differential equations (13) and $n+3$ first-order kinematic differential equations (9). The $(2n+5)$ state variables in the equations of motion are $(\mathbf{q}, \boldsymbol{\nu}) = (x, y, \theta, \theta_1, ..., \theta_n, v, \dot{\theta}, \dot{\theta}_1, ..., \dot{\theta}_n)$. The system is driven by $n-j+3$ actuators including two for the mobile base.

According to the theory of differential flatness [7], [8], we need to select $n-j+3$ flat outputs, equal in number to the control inputs. We choose these $(n-j+3)$ flat outputs to be $(F_1, F_2, F_3, ..., F_{n-j+2}, F_{n-j+3}) = (x, y, \theta_1, ..., \theta_{n-j}, \sum_{i=1}^{n} \theta_i)$.

The differential flatness property with these flat outputs can be shown by expressing all state and input variables in terms of the flat outputs and their derivatives. From the choice of the flat outputs and (9), they are expressed as

$$(x, y, \theta_1, ..., \theta_{n-j}) = (F_1, F_2, F_3, ..., F_{n-j+2}), \tag{16}$$

$$\theta = \arctan\left(\frac{\dot{F}_2}{\dot{F}_1}\right), \ v = \sqrt{\dot{F}_1^2 + \dot{F}_2^2}. \tag{17}$$

The state variables θ_{n-j+1} through θ_n can be written in terms of F_{n-j+3} and its derivatives as follows. Using the special form of the matrices given by (14) and (15) with the choice of the flat output of $F_{n-j+3} = \sum_{i=1}^{n} \theta_i$, the last row

TABLE I

DESIGN CONDITIONS AND FLAT OUTPUTS WITH UNDER-ACTUATED ARMS

• Two-link manipulator ($n = 2$)

# of links with special design	actuator(s)	spring(s)	Flat outputs
$j = 2$	τ_1	k_2	$F_3 = \theta_1 + \theta_2$

• Three-link manipulator ($n = 3$)

# of links with special design	actuator(s)	spring(s)	Flat outputs
$j = 2$	τ_1, τ_2	k_3	$F_3 = \theta_1, F_4 = \theta_1 + \theta_2 + \theta_3$
$j = 3$	τ_1	k_2, k_3	$F_3 = \theta_1 + \theta_2 + \theta_3$

of the equations of motion in (13) is given by

$$a_{n+2}\ddot{F}_{n-j+3} - \frac{1}{2}\dot{\theta}^2(I_{xn} - I_{yn})\sin(2F_{n-j+3}) + k_n\theta_n = 0. \tag{18}$$

Differentiating θ in (17) once and substituting it into (18), one can have θ_n expressed in terms of the flat outputs and their derivatives. Taking advantage of the pattern of the inertia matrix $\mathbf{A}_j$, with the second last row and double derivative of θ_n obtained above, one can solve for θ_{n-1} in terms of the flat outputs and their derivatives. This procedure of differentiation and substitution continues until obtaining the expression for θ_{n-j+2}. Finally, one can express θ_{n-j+1} using $F_{n-j+3} = \sum_{i=1}^{n}\theta_i$ since all the other joint angels are shown to be in terms of the flat outputs and their derivatives. The expression for the joint rate $\dot{\theta}, \dot{\theta}_1, ..., \dot{\theta}_n$ can be obtained by differentiating $\theta, \theta_1, ..., \theta_n$.

In Table I, a set of design conditions is listed with the flat outputs for the mobile manipulator with two- and three-link manipulator arms. In this table, τ_i and k_i denote the actuator and torsion spring at joint i, respectively. The first two flat outputs $(F_1, F_2) = (x, y)$ are common to all the cases. Note that the pattern given in this table applies to manipulators with additional links.

C. Relative Degrees

In order to take advantage of the flatness property for feedback control design by representing the system as a chain of integrators, the *total relative degree* of these flat outputs must be the same as the order of the system, i.e., the number of state variables. On differentiating F_1, F_2 twice, an input appears in the second derivatives, which leads the system to have an ill-defined relative degree. However, by *prolongation* of $\dot{v}$, i.e., considering $\dot{v}$ as an additional state, one gets a well-defined relative degree of 3 for each of F_1 and F_2. However, as one would expect from (18), the third derivative of F_{n-j+3} has a $\ddot{\theta}$ term, that is, an input appears resulting in an ill-defined relative degree. Therefore, in order to have a matched relative degree with the number of state variables, one needs $2j - 3$ prolongation of $\dot{\theta}$. Consequently, additional $2j - 3$ prolongations of $\ddot{v}$ must be done to have a well-matched relative degree of $2j$ for each of F_1 and F_2. Hence, the relative degree of the flat outputs $(F_3, F_4, ..., F_{n-j+2}, F_{n-j+3})$ are respectively $(2, 2, ..., 2, 2j)$. As a result, the total relative degree of the prolonged system is $2n + 4j$ and now matches the order of the prolonged system.

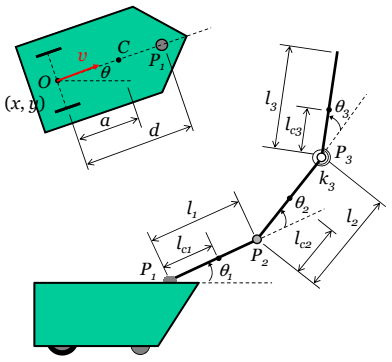

Fig. 2. A mobile vehicle mounted with an under-actuated 3-link manipulator arm. The first two joints P_1 and P_2 have torque inputs and the last joint P_3 is passive with a torsion spring of stiffness k_3

IV. AN ILLUSTRATIVE EXAMPLE

The methodology presented in this paper is illustrated by the mobile manipulator with an under-actuated 3-link arm shown in Fig. 2. In this illustrative example, $n = 3$ and $j = 2$, i.e., the manipulator arm is designed with the following conditions: (i) $l_{c3} = 0$, i.e., the center of mass of the third link is on the third joint P_3; (ii) $m_3 l_2 + m_2 l_{c2} = 0$, i.e., the center of mass of the second and third links together is at the second joint P_2.

The first two joints P_1 and P_2 have torque inputs and the last joint P_3 is passive with a torsion spring of stiffness k_3. With this design, the equations of motion are given by

$$\mathbf{A}_2(\mathbf{q})\dot{\boldsymbol{\nu}} + \mathbf{D}_2(\mathbf{q}, \boldsymbol{\nu}) + \mathbf{G_2}(\mathbf{q}) = \mathbf{J}_2\boldsymbol{\tau}. \tag{19}$$

where

$$\mathbf{A}_2 = \begin{pmatrix} a_{11} & a_{12} & a_{13} & 0 & 0 \\ a_{12} & a_{22} & a_{23} & 0 & 0 \\ a_{13} & a_{23} & a_{33} & a_4 & I_{z3} \\ 0 & 0 & a_4 & a_4 & I_{z3} \\ 0 & 0 & I_{z3} & I_{z3} & I_{z3} \end{pmatrix}, \ \mathbf{G}_2 = \begin{pmatrix} 0 \\ 0 \\ g_3 \\ 0 \\ k_3\theta_3 \end{pmatrix},$$

$$\mathbf{J}_2 = \begin{pmatrix} 1/r & 1/r & 0 & 0 & 0 \\ b/r & -b/r & 0 & 0 & 0 \\ 0 & 0 & 1 & 0 & 0 \\ 0 & 0 & 0 & 1 & 0 \\ 0 & 0 & 0 & 0 & 1 \end{pmatrix}, \mathbf{D}_2 = \begin{pmatrix} d_1 \\ d_2 \\ d_3 \\ d_4 \\ d_5 \end{pmatrix}, \boldsymbol{\tau} = \begin{pmatrix} \tau_r \\ \tau_l \\ \tau_1 \\ \tau_2 \\ 0 \end{pmatrix},$$

$$d_5 = -\frac{1}{2}\dot{\theta}^2(I_{x3} - I_{y3})\sin(2\theta_1 + 2\theta_2 + 2\theta_3).$$

Note that the subscript 2 denotes that the last 2 links have the special inertia distribution suggested in this paper. Detailed expressions for a_{11}, a_{12}, a_{13}, a_{23}, a_{33}, a_4, d_1, d_2, d_3, d_4, and g_3 are not shown here to avoid a lengthy paper. However, note that a_4 is a constant as stated in Section III-A, whereas the other variables are not necessarily constants.

Furthermore, the dynamic model of this system can be expressed in state space form as follows.

$$\dot{\mathbf{q}} = \mathbf{S}\boldsymbol{\nu}, \tag{20}$$

$$\dot{\boldsymbol{\nu}} = \mathbf{f_1} + \mathbf{f_2}\boldsymbol{\tau}, \tag{21}$$

where $\mathbf{q} = [x, y, \theta, \theta_1, \theta_2, \theta_3]^T$, $\boldsymbol{\nu} = [v, \dot{\theta}, \dot{\theta}_1, \dot{\theta}_2, \dot{\theta}_3]^T$, $\mathbf{f_1} = \mathbf{A}_2^{-1}\mathbf{D}_2$ and $\mathbf{f_2} = \mathbf{A}_2^{-1}\mathbf{J}_2$.

A. Construction of Diffeomorphism

In this section, we present the diffeomorphism for the example system. The system's state variables are $(\mathbf{q}, \boldsymbol{\nu}) = (x, y, \theta, \theta_1, \theta_2, \theta_3, v, \dot{\theta}, \dot{\theta}_1, \dot{\theta}_2, \dot{\theta}_3)$. With four actuators, four flat outputs can be selected and they are (F_1, F_2, F_3, F_4) = $(x, y, \theta_1, \theta_1 + \theta_2 + \theta_3)$ as suggested in this paper. The expressions for the state variables in terms of the flat outputs are $(x, y, \theta_1) = (F_1, F_2, F_3)$ and

$$\theta = \arctan\left(\frac{\dot{F}_2}{\dot{F}_1}\right), \; v = \sqrt{\dot{F}_1^2 + \dot{F}_2^2}. \tag{22}$$

The last row of the equations of motion in (19) is given by

$$I_{z3}\ddot{F}_4 - \frac{1}{2}\dot{\theta}^2(I_{x3} - I_{y3})\sin(2F_4) + k_3\theta_3 = 0, \tag{23}$$

so θ_3 can be solved for in terms of the flat outputs and their derivatives.

$$\theta_3 = \frac{1}{k_3}\left\{\frac{1}{2}\left(\frac{\dot{F}_1\ddot{F}_2 - \ddot{F}_1\dot{F}_2}{\dot{F}_1^2 + \dot{F}_2^2}\right)^2 (I_{x3} - I_{y3})\sin(2F_4) - I_{z3}\ddot{F}_4\right\} \tag{24}$$

From the choice of $F_4 = \theta_1 + \theta_2 + \theta_3$, one can solve for θ_2 in terms of the flat outputs and their derivatives using $\theta_1 = F_3$ and the expression for θ_3 in (24). The remaining state variables $\dot{\theta}$, $\dot{\theta}_1$, $\dot{\theta}_2$, $\dot{\theta}_3$ are obtained by differentiating the obtained flat output expressions of θ, θ_1, θ_2, and θ_3. The flat output parametrization for the inputs can be computed using (21). By taking two additional differentiations on $\ddot{F}_4$ from (23), $\ddot{\theta}_3$ appears in the expression of $F_4^{(4)}$. Since it can be found in (21) that $\ddot{\theta}_3$ contains inputs, the relative degree of F_4 is 4 while the relative degree of F_1 and F_2 each is 4 by the prolongation as explained in Section III-C. The relative degree of F_3 is 2. Therefore, the total relative degree is 14 and is well matched with the number of state variables, 14, of the prolonged system, which is added by the three additional state variables.

B. Planning of Desired Trajectories

Initial and final conditions given for the state variables can be mapped to the boundary conditions on the four flat outputs and their derivatives. These boundary conditions are used to generate a smooth trajectory for the flat outputs. Since one can choose a trajectory freely in the flat output space, trajectory planning problem becomes considerably simplified. The inverse mapping is then used to compute the state trajectory from the selected trajectories of the flat outputs.

In this example, the initial conditions of $x(0)$, $y(0)$, $\theta(0)$, $\theta_1(0)$, $\theta_2(0)$, and $\theta_3(0)$ are used to get $F_1(0)$, $\dot{F}_1(0)$, $\ddot{F}_1(0)$, $F_2(0)$, $\dot{F}_2(0)$, $\ddot{F}_2(0)$, $F_3(0)$, $\dot{F}_3(0)$, $F_4(0)$, $\dot{F}_4(0)$, $\ddot{F}_4(0)$, and $\dddot{F}_4(0)$. Similarly, the final conditions, at $t = t_f$, of the flat outputs can be computed from the given final conditions of the state variables. Additionally, one need boundary conditions of v, $\dot{\theta}$, $\dot{\theta}_1$, $\dot{\theta}_2$, $\dot{\theta}_3$, and $\dot{v}$ to match the boundary conditions in flat output space. A smooth trajectory over $t = 0$ and $t = t_f$ is selected that satisfies the boundary conditions that are transformed into the flat output space. In the example, we choose seventh degree polynomials for trajectories of $F_1(t), F_2(t), F_4(t)$ and a third degree polynomial for $F_3(t)$ so that the coefficients of the polynomials can be uniquely determined from the boundary conditions. The desired trajectories over [0,10] sec are planned with the following boundary conditions for $(x, y, \theta, \theta_1, \theta_2, \theta_3)$: (0, 0, 0, 0, 0, 0) at $t = 0$ and $(10, 10, 0, \pi/4, \pi/4, 0)$ at $t = 10$.

C. Controller Design

Due to the flatness property, an exponentially stabilizing controller can be developed in the flat output space since the system is represented by a chain of integrators.

Since the system has four inputs, a subset of (21) can be written as

$$\begin{pmatrix} \dot{v} \\ \ddot{\theta} \\ \ddot{\theta}_1 \\ \ddot{\theta}_3 \end{pmatrix} = \hat{\mathbf{f}}_\mathbf{1} + \hat{\mathbf{f}}_\mathbf{2} \begin{pmatrix} \tau_r \\ \tau_l \\ \tau_1 \\ \tau_2 \end{pmatrix}, \tag{25}$$

where $\hat{\mathbf{f}}_\mathbf{1}$ is the 4×1 subvector of $\mathbf{f_1}$ and $\hat{\mathbf{f}}_\mathbf{2}$ is the 4×4 submatrix of $\mathbf{f_2}$. Then, (25) can be rewritten as

$$\dot{v} = \gamma_1, \tag{26a}$$

$$\ddot{\theta} = \gamma_2, \tag{26b}$$

$$\ddot{\theta}_1 = \gamma_3, \tag{26c}$$

$$\ddot{\theta}_3 = \gamma_4, \tag{26d}$$

using the input transformation

$$\begin{pmatrix} \gamma_1 \\ \gamma_2 \\ \gamma_3 \\ \gamma_4 \end{pmatrix} = \hat{\mathbf{f}}_\mathbf{1} + \hat{\mathbf{f}}_\mathbf{2} \begin{pmatrix} \tau_r \\ \tau_l \\ \tau_1 \\ \tau_2 \end{pmatrix}. \tag{27}$$

In order to find an invertible mapping between the inputs and higher derivatives of the flat outputs, the flat outputs were differentiated until an input appears in their expressions. As we noted in Section III-C, we require two prolongations of $\gamma_1 (= \dot{v})$, and one prolongation of γ_2 resulting in three additional state variables to the system. This makes the number of state variables of the system to be 14. Then, one gets

$$\begin{pmatrix} F_1^{(4)} \\ F_2^{(4)} \\ \ddot{F}_3 \\ F_4^{(4)} \end{pmatrix} = \begin{pmatrix} C_1 \\ C_2 \\ C_3 \\ C_4 \end{pmatrix} + \begin{pmatrix} c_\theta & -vs_\theta & 0 & 0 \\ s_\theta & vc_\theta & 0 & 0 \\ 0 & 0 & 1 & 0 \\ 0 & D_{42} & 0 & -\frac{k_3}{I_{z3}} \end{pmatrix} \begin{pmatrix} \ddot{\gamma}_1 \\ \dot{\gamma}_2 \\ \gamma_3 \\ \gamma_4 \end{pmatrix}, \tag{28}$$

where c_θ denotes $\cos\theta$, s_θ $\sin\theta$, and $D_{42} = \frac{1}{I_{z3}}\dot{\theta}(I_{x3} - I_{y3})\sin(\theta_1 + \theta_2 + \theta_3)$. The entries C_i are not shown here to avoid a lengthy paper, but they are a function of the state variables of the prolonged system. From this relation, one

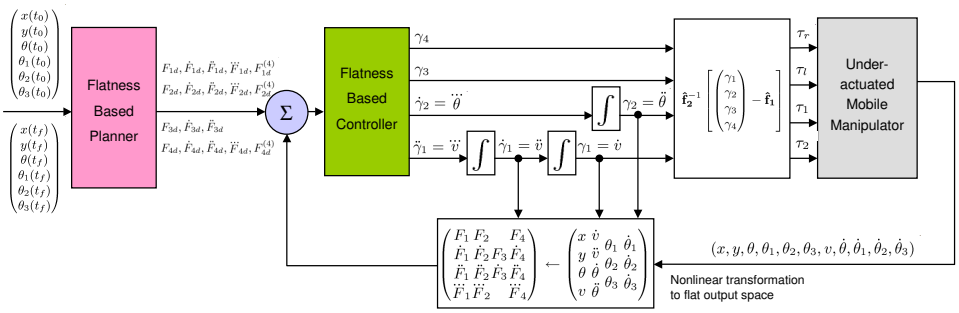

Fig. 3. The integrated planner and controller with the dynamic model of the mobile manipulator.

observes that the total relative degree of the prolonged system becomes 14, which is well matched with the order of the prolonged system. Therefore, in the flat output space, the system is governed by the linear equations with new inputs u_1, u_2, u_3, and u_4 such that

$$F_1^{(4)} = u_1,\ F_2^{(4)} = u_2,\ \ddot{F}_3 = u_3,\ F_4^{(4)} = u_4. \tag{29}$$

In order to achieve exponentially stable tracking control, u_1, u_2, u_3, and u_4 are selected as

$$u_1 = F_{1d}^{(4)} + p_3\dddot{\tilde{F}}_1 + p_2\ddot{\tilde{F}}_1 + p_1\dot{\tilde{F}}_1 + p_0\tilde{F}_1, \tag{30a}$$

$$u_2 = F_{2d}^{(4)} + q_3\dddot{\tilde{F}}_2 + q_2\ddot{\tilde{F}}_2 + q_1\dot{\tilde{F}}_2 + q_0\tilde{F}_2, \tag{30b}$$

$$u_3 = \ddot{F}_{3d} + r_1\dot{\tilde{F}}_3 + r_0\tilde{F}_3, \tag{30c}$$

$$u_4 = F_{4d}^{(4)} + s_3\dddot{\tilde{F}}_4 + s_2\ddot{\tilde{F}}_4 + s_1\dot{\tilde{F}}_4 + s_0\tilde{F}_4, \tag{30d}$$

where $\tilde{F}_i$ is defined as $F_{id} - F_i$ and F_{id} denotes the desired trajectory of the flat output F_i. p_i, q_i, r_i, and s_i are control gains that are chosen appropriately such that all roots of the characteristic equations of the closed loop error dynamics lie in the left half-plane to ensure exponential stability.

On substituting (30) into (29), one can compute $\ddot{\gamma}_1$, $\dot{\gamma}_2$, γ_3, and γ_4 from (28). γ_1 and γ_2 can then be obtained by integration. The original torque inputs τ_r, τ_l, τ_1, and τ_2 are then computed using (27).

D. Simulation Results

The block diagram for the planner and controller is presented in Fig. 3. Figure 4 (a) shows the desired and actual trajectories of the mobile base's coordinates (x, y). In this simulation, initial errors were given by taking the initial conditions for $y(0)$, $\theta_1(0)$, $\theta_2(0)$, and $\theta_3(0)$ as 1.0 m, $\pi/6$ rad, $\pi/6$ rad, and $\pi/6$ rad, respectively in order to check the exponential convergence to the desired trajectory. The control gains in (30) were chosen in a way that all the roots of the characteristic equations of the error dynamics are all at -3. The desired and actual trajectories of θ, θ_1, θ_2, and θ_3 are shown in Fig. 4 (b). The system parameters used in the simulation are: $(d, a, r, b, l_1, l_2, l_3) = (1, 0.5, 0.3, 0.5, 1, 1, 1)$ m, $(m_0, m_1, m_2, m_3) = (5, 1, 1, 1)$ kg, $(I_0, I_1, I_2, I_3) = (5, 1, 1, 1)$ kg·m^2, and $k_3 = 1$ N·m/rad.

V. Conclusion

In this paper, it was shown that mobile manipulators with an under-actuated vertical arm can also be made differentially flat using the inertia redistribution design methodology

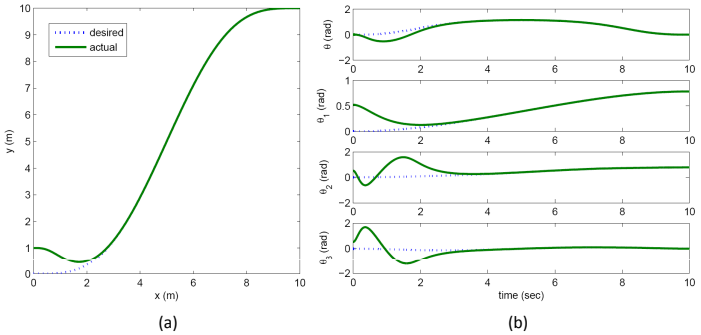

Fig. 4. (a) The mobile base's desired and actual trajectories. (b) The desired and actual trajectories for θ, θ_1, θ_2, and θ_3.

introduced in the previous studies [3], [4]. As a result, a wide range of differentially flat designs can be achieved. The differential flatness property significantly simplifies trajectory planning and feedback control. The proposed method was illustrated by the example of a mobile manipulator with a three-link vertical under-actuated arm. Simulation results were presented to verify point-to-point maneuvers of the system satisfying the dynamic model with nonholonomic constraints and under-actuation, while ensuring exponential stability.

References

[1] Z. Li, A. Ming, N. Xi, and M. Shimojo, "Motion control of nonholonomic mobile underactuated manipulator," in *Proc. IEEE Int. Conf. on Robotics and Automation*, 2006, pp. 3512–3519.

[2] K. Kobayashi and T. Yoshikawa, "Controllability of under-actuated planar manipulators with one unactuated joint," *Int. J. of Robotics Research*, vol. 21, no. 5-6, pp. 555–561, 2002.

[3] J.-C. Ryu, V. Sangwan, and S. K. Agrawal, "Differentially flat designs of underactuated mobile manipulators," *ASME Transactions, J. of Dyn. Sys. Meas. and Control*, vol. 132, no. 2, p. 024502, 2010.

[4] J.-C. Ryu and S. K. Agrawal, "Planning and control of under-actuated mobile manipulators using differential flatness," *Autonomous Robots*, 2010, submitted.

[5] S. K. Agrawal and A. Fattah, "Reactionless space and ground robots: novel designs and concept studies," *Mechanism and Machine Theory*, vol. 39, no. 1, pp. 25–40, 2004.

[6] S. K. Agrawal and V. Sangwan, "Differentially flat designs of under-actuated open-chain planar robots," *IEEE Trans. on Robotics*, vol. 24, no. 6, pp. 1445–1451, 2008.

[7] M. Fliess, J. Levine, P. Martin, and P. Rouchon, "Flatness and defect of non-linear systems: Introductory theory and examples," *Int. J. of Control*, vol. 61, no. 6, pp. 1327–1361, 1995.

[8] H. Sira-Ramirez and S. K. Agrawal, *Differentially Flat Systems*. New York: Marcel Dekker, 2004.